

The investigation of mixed monolayers adsorbed from solution: octane and nonane mixtures on graphite†

Miguel A. Castro,^a Stuart M. Clarke,^{*b} Akira Inaba,^c Thomas Arnold^d and Robert K. Thomas^d

^a Instituto de Ciencia de Materiales de Sevilla, Avda, Americo Vespucio, Sevilla, Spain

^b Cavendish Laboratory, Madingley Road, Cambridge, UK, CB3 0HE,

^c Department of Chemistry and Research Centre for Molecular Thermodynamics, Graduate School of Science, Osaka University, Toyonaka, Osaka 560-0043, Japan

^d Physical and Theoretical Chemistry Laboratory, South Parks Road, Oxford, UK OX1 3QZ

Received 30th July 1999, Accepted 16th September 1999

The combination of sensitive calorimetry, incoherent elastic neutron scattering and neutron diffraction has been used to demonstrate the formation of solid layers containing both octane and nonane adsorbed onto graphite from the binary alkane mixture. This combination of methods allow us to characterise the adsorbed layer in some detail including the absolute composition and melting temperature as a function of solution composition. The evidence presented here suggests that the two alkanes exist on the surface as patches of pure material not as a single crystal incorporating both alkanes.

Introduction

The presence of solid monolayers of simple alkanes, alcohols and carboxylic acids adsorbed from solution to a solid surface, typically graphite, has been a significant issue for many years. The early calorimetry and isotherm measurements^{1–4} suggested that the adsorption was sufficiently strong that ordered layers could be formed. These monolayers have a role in many important interfacial phenomena, but their characterisation is difficult, largely because of the presence of the solution. Recently structural information from techniques such as specular neutron reflectivity⁵ and scanning tunnelling microscopy (STM)⁶ has started to become available. However, reflectivity measurements only provide structural information normal to the plane of the interface and there is still often significant uncertainty over the interpretation of the results from STM techniques. Recently we have developed the more direct methods of incoherent elastic neutron scattering⁷ and coherent neutron diffraction^{8–10} to clearly identify the presence of solid monolayers adsorbed from solution and provide crystallographic detail of their structures. Neutron diffraction has been used previously to investigate the adsorption of solid monolayers of pure alkanes.^{11–13} These techniques have the sensitivity to distinguish the surface layer from the bulk phases while minimising the problem of obtaining adequate transmission. With techniques such as these, which are not surface specific, it is desirable to enhance the relative contribution from the adsorbed layer by using powdered, high specific surface area substrates and to reduce the quantity of bulk solution phase to a minimum. Previous calorimetry measurements on related systems indicate that the minimum amount required to have the characteristics of the true bulk solution phase is of the order of 5–10 monolayers.¹⁰

Incoherent elastic neutron scattering is a powerful tool for the investigation of monolayers adsorbed from pure materials and solutions^{7,8} providing unambiguous information on both the state and absolute composition of an adsorbed layer and

the surface area per molecule on the surface. Significantly, this technique is able to distinguish the individual behaviour of each component of multicomponent solutions⁸ even when the components are as similar as octane and nonane. Neutron scattering techniques are time consuming and difficult measurements to make so calorimetry has been used in this work to survey the temperature and composition behaviour to target neutron measurements.

In our previous work we have employed binary mixtures of alkanes and long chain carboxylic acids⁸ and binary mixtures of alkanes of different lengths.¹⁰ In these cases one component was much more strongly adsorbed than the other, principally due to the differences in chain length with the longer molecules more strongly adsorbed. In this work we consider molecules that are very similar in length, octane (C₈), and nonane (C₉), over a wide concentration range. Because the strength of adsorption of the two molecules is similar, we may expect more effective competitive adsorption and a behaviour that is sensitive to solution composition.

In this paper the adsorption behaviour of the binary mixtures of the linear alkanes, octane (C₈) and nonane (C₉) on graphite are investigated using incoherent elastic neutron scattering (IQNS) in combination with calorimetry and neutron diffraction. Two calorimetry methods have been used, differential scanning calorimetry (DSC), to characterise these materials over a wide range of composition, coverage and temperature and adiabatic calorimetry, a more accurate method, to address particular compositions of interest in more detail. Incoherent elastic neutron scattering measurements confirm the presence of solid adsorbates and allow determination of the absolute composition of the monolayers. Neutron diffraction also confirms the formation of solid monolayers, provides an independent estimate of composition and provides a means of characterisation of the structure of the mixed monolayer observed.

Experimental

Only a brief outline of the IQNS, calorimetry and neutron diffraction techniques are presented here; full details can be found elsewhere.

† Contribution No. 6 from the Research Centre for Molecular Thermodynamics.

IQNS

The experimental approach is based on the underlying principle that the intensity of incoherent elastic scattering depends upon the quantity of solid material present in the sample cell.^{9,10} This technique is sufficiently sensitive to observe submonolayer quantities of solid material even in the presence of significant quantities of liquid or solution. In this work we are principally concerned with the evolution of the elastic scattering intensity with temperature and, as discussed previously,¹⁰ the high resolution of the instrument IN10 at the Institut Laue-Langevin, Grenoble, France, enables us to obtain this information directly. The intensity of incoherent scattering is particularly strong for protons, even relative to deuterons, which means that isotopic labelling can be used to investigate individual components of multicomponent systems.⁸

In these experiments each sample of graphite is dosed with one alkane and then the other alkane is sequentially added to sweep the mole fraction of the mixture. During this experiment two shapes of sample can were employed. Initially a flat can was used to optimise the illuminated volume of sample without causing transmission problems. However, it proved difficult to replace and orient the sample, after dosing with alkanes, in a repeatable fashion leading to a small but significant variation in scattering level and background. Subsequently a cylindrical can was used, which enabled a much more reliable repositioning of the sample after dosing with very repeatable scattering and background levels. The measured transmission of the dosed samples was approximately 80% in both cases.

Differential scanning calorimetry (DSC)

The DSC measurements were performed on two Perkin-Elmer DSC7 systems at the Polymers and Colloids Group, Cavendish Laboratory and at the Department of Materials Science and Metallurgy, both at the University of Cambridge, as discussed previously.¹⁰ The minimum temperatures accessible with these instruments were -65°C and -130°C , respectively. The heating rate used was $10^{\circ}\text{C min}^{-1}$.

Adiabatic calorimetry

The method and experimental details of adiabatic calorimetry have been presented in detail elsewhere.¹⁴ Essentially, the heat capacity of a sample of substrate (graphite) dosed with a known amount of adsorbate is directly determined as a function of temperature by adding tiny amounts of electrical heating energy to the sample and measuring the temperature rise. Transitions are indicated as peaks in the heat capacity.

Neutron diffraction

The neutron diffraction measurements presented here were performed on the OSIRIS instrument at ISIS, Rutherford Appleton Laboratory, Chilton, Didcot, Oxfordshire, UK. Pulses of neutrons from the source, *via* a methane moderator, are selected into wavelength batches by two choppers and are scattered by the sample to a bank of detectors in an almost back scattering geometry. This geometry gives high resolution. The wavelength of the scattered neutrons is determined from their time of flight.

Samples

The recompressed exfoliated graphite, Papyex (Le Carbone Lorraine), was used as adsorbent in these experiments with a specific surface area¹⁰ of $14\text{ m}^2\text{ g}^{-1}$. Protonated alkanes were obtained from Aldrich, and purified by passage through an alumina column (Brockmann I, activated, basic). Deuterated nonane was obtained from Cambridge Isotope Laboratories

and deuterated octane from Aldrich, both with a quoted deuteration level of $>99\%$. The graphite substrates were outgassed under vacuum in an oven before known quantities of the adsorbates were added as liquid and annealed at a temperature just below the bulk boiling point.

It is convenient to prepare samples with coverages in terms of a number of equivalent monolayers. This requires estimates of the surface area per molecule (octane 52.4 \AA^2 and nonane 57.6 \AA^2)⁴ and the specific surface area of the particular sample of graphite ($14\text{ m}^2\text{ g}^{-1}$). From now on we refer to equivalent monolayers as monolayers. The solution composition will depend upon the composition of the adsorbed monolayer if it has a different composition to the solution. However, where there are reasonable quantities of bulk solution present the adjustment of the concentration by adsorption is small. In this work we make the approximation that the solution composition is unchanged by adsorption.

For the DSC measurements approximately 20 mg of graphite was used dosed with fully protonated materials. The total coverage was in excess of 40 monolayers. Approximately 10 g of graphite was dosed with fully deuterated materials for the neutron diffraction measurements to reduce the incoherent scattering that would have arisen if protonated materials were used. Mixtures of both protonated and deuterated alkanes were used for the IQNS measurements as discussed below. In the adiabatic calorimetry 9.21 g of graphite was dosed with adsorbate (10 equivalent monolayers of octane required 475 mg and 10 equivalent monolayers of nonane 477 mg).

Results

Differential scanning calorimetry

Fig. 1 shows the DSC thermogram for a mixture of octane and nonane adsorbed on graphite at mole fraction of octane (X_{oct}) of 0.75 and a total coverage equivalent to about 40 monolayers. The graphs are plotted such that an upward peak corresponds to an endothermic transition. Over the temperature range investigated here there are no features in the DSC thermogram of graphite alone. By comparison of DSC thermograms with and without graphite, the two peaks in Fig. 1 at the lowest temperatures can be shown to arise from the bulk solution. Note that at this high coverage the temperature of the bulk transitions are identical whether or not graphite is present. This would not necessarily be the case at lower total coverages.¹⁰ Since the highest temperature peak only appears when both graphite and alkanes are present, it must be associ-

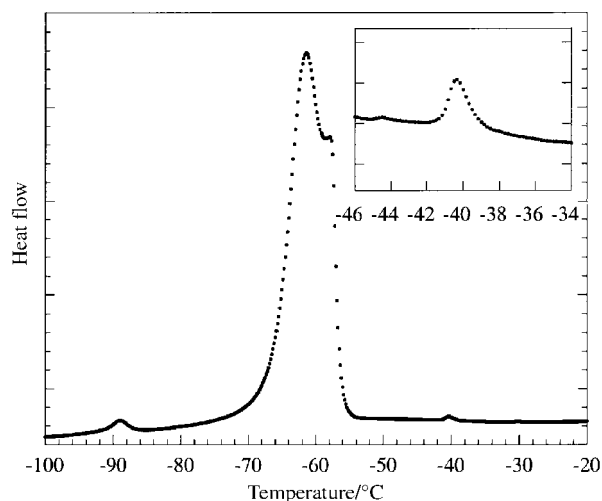


Fig. 1 DSC thermogram of octane and nonane mixture, with $X_{\text{oct}} = 0.75$, on graphite. Upward peaks correspond to endothermic transitions. The inset shows the monolayer transition region in more detail.

ated with an adsorbed layer. The results of measurements at the same total coverage but over the full range of solution composition are summarized in Fig. 2.

Bulk behaviour. The higher of the two bulk transitions is taken to be the bulk melting point. Starting with one pure component, this shows the expected depression in freezing point as the other component is added. Over the composition range from about $X_{\text{oct}} = 0.45$ to 0.75 this melting point is approximately constant. The lower temperature transition moves to a lower temperature with increased mole fraction of octane. The peak magnitude for this second transition decreases with increasing octane mole fraction until it cannot be observed at X_{oct} of approximately 0.8. For compositions between about 0.3 and 0.9 (X_{oct}) the higher of the two peaks also has a low temperature shoulder, which, over the range that we can observe it, occurs approximately at 212 K. It is tempting to attribute this to a eutectic line but there are strong reasons for supposing that it is not, and we return to this below.

Pure bulk nonane forms a rotator phase just before melting¹⁵ and we interpret the lowest temperature transition for pure nonane in Fig. 2 as a transition to this rotator phase. The range of stability of rotator phases is generally found to be enhanced by additives¹⁶ and this behaviour is also unambiguous in Fig. 2 as octane is added. Pure octane, however, does not form a rotator phase¹⁵ and it is therefore not surprising that the rotator phase transition weakens and eventually disappears at high octane mole fractions. The most important consequence of the variation of the temperature of transition to the rotator phase with composition is that it must mean that octane forms a solid solution in nonane over the composition range over which this temperature variation is observed. It is this observation that makes it impossible that the shoulder at about 212 K is associated with a eutectic line. For a eutectic to exist there has to be a two-phase region at temperatures below the eutectic temperature. The consequence of this is that over a significant range of composition around the eutectic composition the two phases have to have a fixed composition and one of these phases is the rotator phase. However, the rotator phase transition shows quite unambiguously that the composition of the rotator phase in this region of composition is varying continuously. Hence,

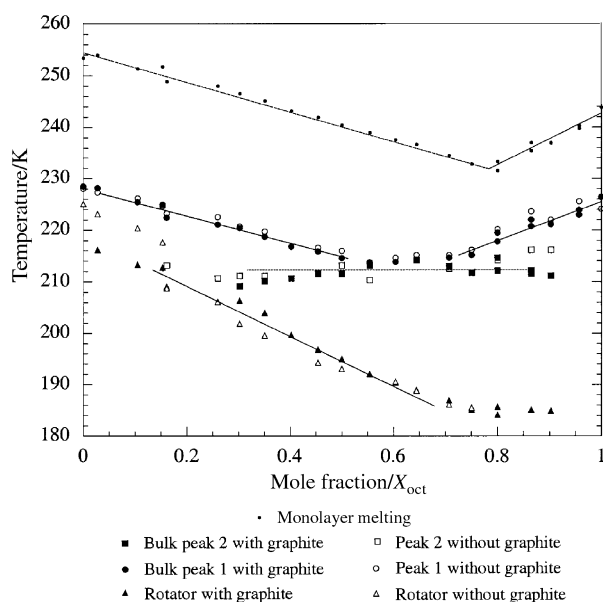


Fig. 2 Coverage and temperature dependence of the bulk and monolayer transitions of octane and nonane mixtures on graphite. The figure includes transitions observed with and without the graphite substrate used to identify bulk transitions. Lines are provided as guides to the eye.

octane and nonane in the bulk do not form a eutectic. A phase diagram that is consistent with all the data is shown schematically in Fig. 3. It indicates that bulk nonane and octane form a continuous range of solid solutions. The presence of the minimum in the melting temperature of the mixture indicates that mixing in the solid state is not ideal. Evidently, the disparity in size is sufficient to cause some non-ideality.

The phase behaviour of other binary mixtures of shorter alkanes differing in chain length by one CH_2 unit has been reported.¹⁷ In each of the systems reported ($\text{C}_{11}/\text{C}_{12}$, $\text{C}_{12}/\text{C}_{13}$, $\text{C}_{13}/\text{C}_{14}$, $\text{C}_{14}/\text{C}_{15}$ and $\text{C}_{15}/\text{C}_{16}$) the crystal structures of the two alkanes differ, being orthorhombic ('odd') and triclinic ('even'), and the phase diagrams clearly exhibit non-ideal behaviour. The phase diagrams of $\text{C}_{12}/\text{C}_{13}$ and $\text{C}_{14}/\text{C}_{15}$, are qualitatively similar, *e.g.*, exhibiting a pronounced minimum in the melting curve and the same behaviour of the onset of a rotator phase, to that determined here for octane and nonane, even though the bulk crystal structures of octane and nonane are both triclinic. It is interesting that in another binary alkane mixture (C_{19} and C_{21}) mixing is ideal but can be made non-ideal (*i.e.*, a temperature minimum) by going to high pressures.¹⁸

Monolayer transitions. The heat capacity peak at temperatures above the bulk melting point in Fig. 1 can be attributed to a transition of an adsorbed layer. As for the bulk material the transition temperature falls from either pure component giving rise to a pattern that more closely resembles eutectic formation than did the bulk, but with an apparent eutectic composition richer in octane. The greater resemblance to a eutectic is that the decline of temperature towards the apparent eutectic is greater and sharper than was found for the bulk melting point. It is important to note that DSC is unable to distinguish which component or mixture of components is adsorbed at any composition, except at the limits of the pure single components. The value of such a eutectic temperature would, of course, be the true eutectic temperature, but the eutectic composition would be undetermined because we do not know the composition of the adsorbed layer, only the total. Although the form of the adsorbed monolayer melting point behaviour suggests eutectic behaviour, the DSC data does not show the eutectic line. Thus, at all compositions, a phase diagram with a eutectic should show a small phase transition at the eutectic temperature. However, for a monolayer, this would demand a high experimental sensitivity.

For a first-order bulk melting transition the best estimate of the transition temperature in a DSC trace is the temperature at which the onset of the transition occurs, while for higher order transitions, which may occur for monolayer melting, it is the value at the peak maximum. The uncertainty in the

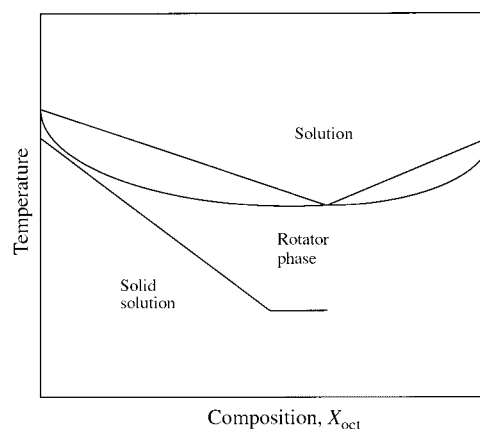


Fig. 3 Schematic phase diagram of the bulk and monolayer behaviour of octane and nonane mixtures adsorbed on graphite.

transition temperatures determined by DSC arises from the temperature calibration of the instrument and the extrapolation procedure used to find the onset temperature. In Fig. 2 we have given peak positions for all transitions, all of which will be relatively high, and we estimate the error to be about 5 K.

Adiabatic calorimetry

Adiabatic calorimetry is a very labour intensive experiment and therefore we only examined a small selection of conditions for investigation. In general, the transitions reported above using DSC agree with those observed with adiabatic calorimetry measurements. However, the adiabatic calorimetry data were recorded using long equilibration times and, not surprisingly, some extra transitions are observed. Here we only present the additional information obtained with adiabatic calorimetry. Fig. 4 presents adiabatic calorimetry data from a mixture of octane and nonane at a mole fraction of $X_{\text{oct}} = 0.6$ in the region of the transition in the adsorbed monolayer. There are now two peaks evident in this region whereas only one was present in the DSC. Allowing for the uncertainty in the temperature of the transition from the DSC measurements, the upper of the two peaks seen in adiabatic calorimetry is almost certainly the melting point of the adsorbed monolayer. The lower peak corresponds to a transition about 10 K below the melting temperature and could be associated with a eutectic line. Unfortunately, we can not make an unambiguous assignment of this peak for reasons that will become clear below.

Fig. 5 presents adiabatic calorimetry data from (a) pure nonane and (b) pure octane adsorbed on graphite at a coverage of ten equivalent monolayers. The adiabatic calorimetry results at this coverage contain several features. The bulk melting point of nonane at 219 K is evident as a large peak. However, there are now three peaks above this temperature, not present for pure nonane in the absence of graphite, which we therefore assign to an adsorbed monolayer. It is difficult to interpret these three transitions but it is probable that the one at highest temperature is associated with melting of the adsorbed monolayer. The lower ones must then be solid/solid transitions in the monolayer, such as the formation of rotator or hexatic phases. For pure octane on graphite, Fig. 5(b) there are just two peaks associated with the adsorbed layer and, again, the higher of the two is probably associated with melting. It is the presence of these other transitions in the monolayer that makes it impossible to be certain that the lower transition observed at a composition of $X_{\text{oct}} = 0.6$ is associated with a eutectic line. Adiabatic calorimetry data

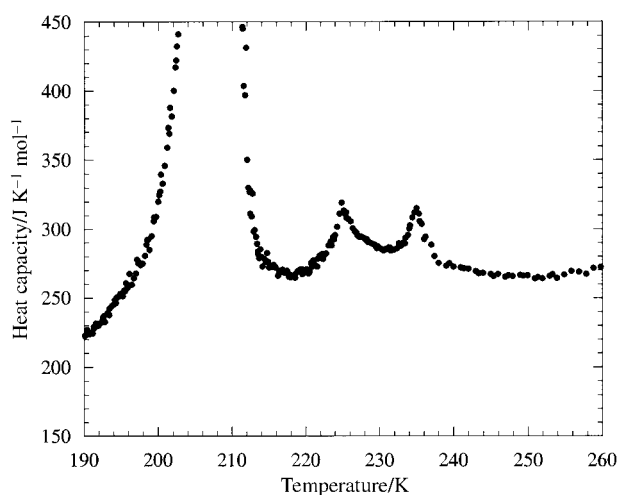


Fig. 4 Adiabatic calorimetry measurements from a mixture of octane and nonane, with a mole fraction, X_{oct} , of 0.6 adsorbed on graphite in the monolayer region.

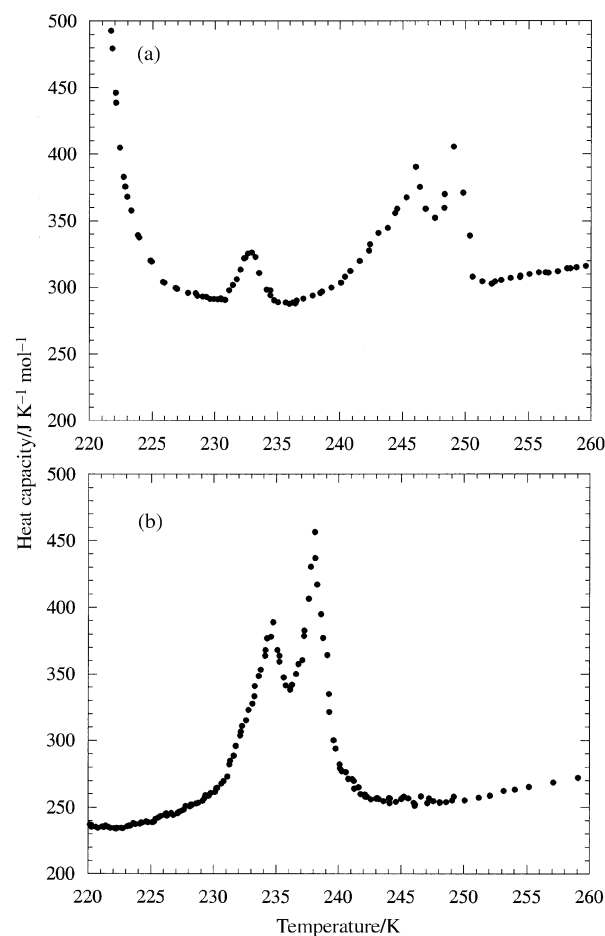


Fig. 5 Adiabatic calorimetry measurements from 10 equivalent monolayers of (a) pure nonane and (b) pure octane adsorbed on graphite in the monolayer region.

obtained at $X_{\text{oct}} = 0.8$ showed only a single monolayer peak, which would be consistent with either a eutectic (and 2D solid phase separation) or with a continuous series of solid solutions.

Incoherent elastic neutron scattering

As discussed above, the contributions from protonated components will dominate the incoherent scattering; the contribution from the deuterated components will always be relatively small. To examine the separate components of the mixture, combinations of protonated and deuterated molecules, such as mixtures of d-octane, C_8D_{18} , with h-nonane, C_9H_{20} (scattering predominantly from the nonane), and h-octane, C_8H_{18} , with d-nonane, C_9D_{20} , (scattering predominantly from the octane), were used. By this means the amount of solid octane and nonane at each temperature could be determined separately.

The actual contribution to the incoherent elastic scattering from each component depends upon the incoherent cross-section of the individual molecules. The actual protonated samples used in this work are taken to be fully protonated. However, the level of deuteration is important because even a small amount of protonated material will greatly increase the incoherent scattering from that component. Table 1 gives the incoherent scattering cross-sections from the protonated and deuterated alkanes used in this work and this takes into account the true extent of deuteration. The contribution of the deuterated component to the scattering can then be calculated for the mixtures used. It is estimated that the deuterated component will account for approximately only 10% of the total scattering when present at even twice the mole fraction of the protonated component.

Table 1 Incoherent cross-sections for the materials used in this work

Molecule	Incoherent cross-section/b ^a	
	Protonated material	Deuterated material
Octane	1438	64.76
Nonane	1598	71.96

^a 1 b (barn) = 10⁻²⁸ m².

Fig. 6 shows the intensity of the incoherent elastic peak as a function of temperature for a fixed quantity of h-octane and increasing amounts of d-nonane in the sample cell. For the case of pure h-octane at the lowest temperatures all the octane is solid giving a strong elastic signal. As the bulk melting point (216 K) is approached and crossed the intensity falls significantly. However, above the bulk melting temperature there is still a significant residual intensity. At this temperature this residual intensity cannot arise from bulk solid material and must therefore result from the presence of immobile adsorbed species. We have discussed the timescale of this immobility in previous papers.^{9,10} For the purposes of our discussion here, it means solid-like material. The residual intensity from the solid adsorbed layer is maintained to higher temperatures when the adsorbed layer melts and the elastic scattering falls to the level of the graphite background. The melting temperatures of the adsorbed layer can be estimated from these figures based on the position of the end of the monolayer plateau. The level of scattering expected for a solid monolayer of h-octane can be estimated, based on the level of scattering at low temperatures when all the octane is solid, the specific surface area of the graphite (14 m² g⁻¹) and the area per molecule.⁴ This level of scattering for a monolayer is illustrated in Fig. 6 and is in reasonable agreement with the level of the monolayer plateau observed. This simple calculation suggests that there is only a single layer adsorbed on the graphite and that the molecules are predominantly lying with their long axes parallel to the graphite surface, since Groszek's estimate of the area per molecule was based on this molecular orientation.

The scattering, represented by other data sets in Fig. 6 for the same quantity of h-octane and increasing quantities of d-nonane, is still dominated by the contribution from the proto-

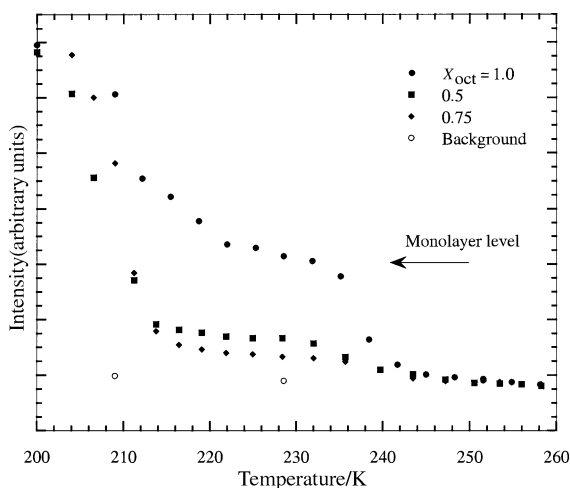


Fig. 6 Incoherent elastic neutron scattering as a function of temperature for solutions of different compositions of h-octane and d-nonane adsorbed on graphite, $X_{\text{oct}} = 1.0, 0.75$ and 0.5 . The scattering in this figure is dominated by the contribution from the protonated octane. The arrow indicates the intensity of scattering expected from a solid monolayer of pure octane. The various transitions are discussed in the text. This data was obtained at a momentum transfer, Q , of 1.416 \AA^{-1} , where Q is defined here as $(4\pi\sin\theta)/\lambda$ where λ is the neutron wavelength (0.6275 nm) and θ is half the scattering angle.

nated octane. Although these curves show similar qualitative features, they differ in several important respects, most importantly, the level of scattering at the monolayer plateau is falling with increasing nonane concentration. This clearly indicates that the amount of octane in the solid monolayer is falling. Thus, the longer alkane, nonane, progressively displaces octane from the surface with increasing nonane concentration in the solution. Assuming that each octane molecule adopts the same area per molecule as in the pure octane monolayer we can estimate the fraction of the monolayer occupied by octane as a function of solution composition, as illustrated in Fig. 7(a). The monolayer transition temperatures are in good agreement with the calorimetry measurements. The IQNS results confirm that the transitions observed in the calorimetry are associated with melting of the adsorbed layers.

Similar data taken with h-nonane with increasing amounts of d-octane exhibit similar features where the initially complete monolayer of nonane is gradually replaced by octane. However, these measurements, unlike those for the h-octane case, were made in a flat can and the quantitative estimates of the amounts of nonane in the solid monolayer, given in Fig. 7(b), are considered to be less reliable. In the case of pure nonane, only a single monolayer transition is evident.

Neutron diffraction

The neutron diffraction patterns from mixtures of octane and nonane on graphite are given in Fig. 8 with mole fractions (X_{oct}) of 0.0, 0.6 and 1.0. The temperatures have been selected to be approximately 10 °C above the bulk melting point at

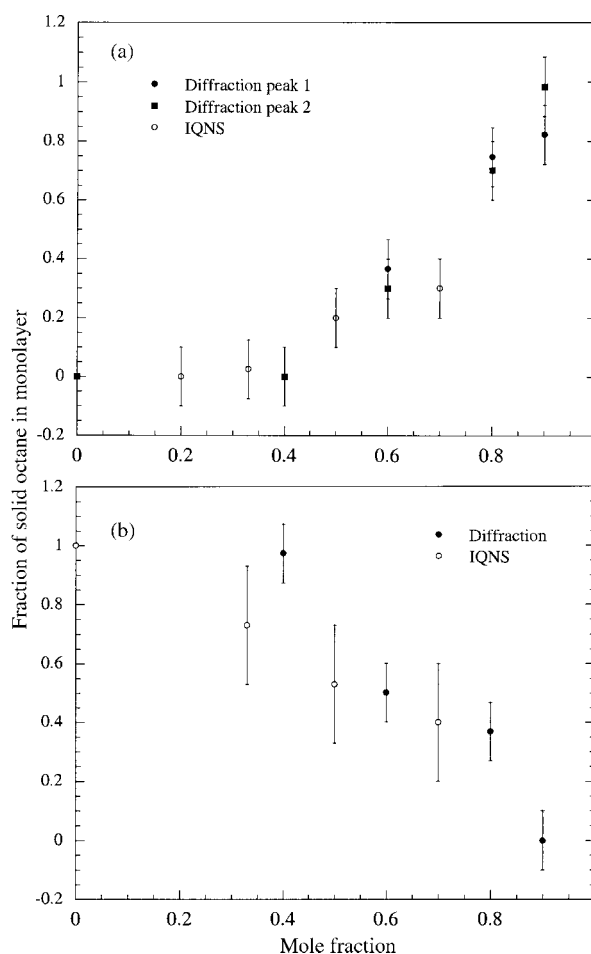


Fig. 7 Composition dependence of the solid monolayer formed by octane and nonane as a function of solution composition. (a) Amount of solid octane and (b) amount of solid nonane in the monolayer. This figure includes data from both incoherent neutron scattering and neutron diffraction.

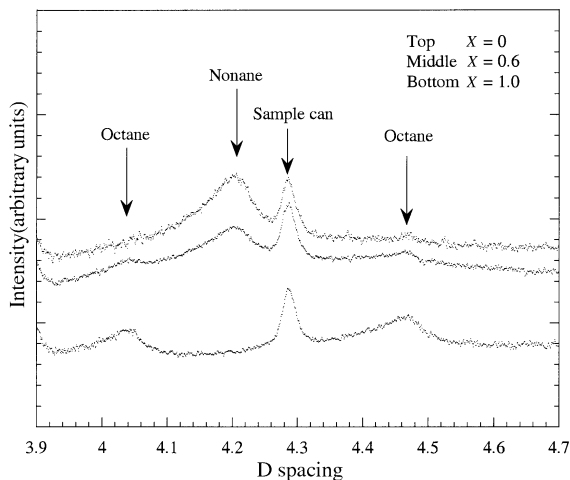


Fig. 8 Neutron diffraction patterns from mixtures of octane and nonane of different composition with X_{oct} of 0.0 (top), 0.6 (middle) and 1.0 (bottom). The arrows indicate the monolayer peaks, as discussed in the text, and a peak from the sample can.

that composition. A peak arising from scattering by the sample can is also identified in this figure. The diffraction pattern from pure nonane on graphite, top data set in Fig. 8, has an additional peak, relative to the background and indicated by the arrow, arising from the solid monolayer of pure nonane. There is also a very broad peak from the fluid nonane underneath this sharper reflection. The adsorbed layer peak is asymmetric, rising sharply at high d -spacing and falling slowly to low d -spacing, a characteristic of two-dimensional monolayers.^{19,20}

The diffraction pattern from adsorbed octane also given in Fig. 8 shows two additional peaks, relative to the background, arising from the solid monolayer of pure octane. These are again indicated by arrows in Fig. 8.

The diffraction pattern at the composition X_{oct} of 0.6, Fig. 8 middle data set, and observed at the other compositions investigated ($X_{\text{oct}} = 0.4, 0.8$ and 0.9), not shown, contain peaks characteristic of both octane and nonane monolayers which coexist. There is no evidence of displacement of these peaks with solution composition suggesting that no mixed crystal is formed but rather patches of pure nonane and pure octane coexist on the surface together. This again strongly indicates that the monolayers behave as a eutectic mixture. The relative intensity of the peaks can be used to estimate the composition of the solid monolayer with solution composition. In this calculation we have taken the intensity of the peaks with pure nonane and pure octane to be complete monolayers. The results of this calculation are presented in Fig. 7(a) and (b) and are seen to be in good agreement with the values determined by IQNS. If the solid monolayer is simply a replacement of octane by nonane or *vice versa* then the total fractional coverage should always be unity. Within the errors of the measurement the sum is indeed unity.

Additional scattering patterns, not shown, from 8 monolayers of pure nonane below the bulk melting point at 200 K and 212 K also were collected. It is observed that on passing through the transition temperature several diffraction peaks from the nonane become a single peak consistent with a structural transition from a low symmetry to higher symmetry structure. These patterns are thus consistent with the hypothesis that the lowest temperature bulk transition in Fig. 1 is the onset of a rotator phase.

Discussion and conclusions

The incoherent elastic neutron scattering measurements demonstrate the competitive adsorption of octane and nonane

on graphite resulting in the formation of a solid monolayer containing both octane and nonane with a composition that depends upon the solution concentration. It is found that the longer alkane, nonane, is preferentially adsorbed unless there is a significant excess of octane in the solution.

The results from the incoherent elastic scattering and calorimetry experiments on these alkane mixtures presented here extend our earlier work^{7,9,10,14} and indicate that only single solid monolayers are adsorbed, in contrast to other workers who reported the formation of more than one solid monolayer in pure alkanes adsorbed on graphite.^{21,22} The DSC and IQNS results show reasonable agreement in the melting temperatures of the monolayers.

The results presented here also indicate the formation of monolayers with molecules lying with their long axis parallel to the surface. Other recent diffraction studies also support this model of molecules lying flat on the surface but highlight a particular difference in the crystal structures of 'odd' and 'even' alkanes adsorbed on graphite.²³ 'Even' members have solid monolayers crystal structures with a zig-zag arrangement of molecules, *pgg* space group, in contrast to the 'odd' alkanes, *e.g.*, heptane, in which the molecules all lie parallel to each other. However, dodecane is an exception and forms a monolayer where molecules lie parallel to one another.²³ Kitaigorodskii has discussed the importance of symmetry in the formation of mixed crystals.²⁴ In simple terms, two molecules that have different crystal symmetries will not form mixed crystals but eutectics.

Other workers have identified the formation of ordered monolayers of pure alkanes adsorbed onto graphite at sub-monolayer and multilayer coverages including the zig-zag arrangement of molecules parallel to the graphite surface for butane¹¹ and hexane.^{12,13} However, the melting point of the butane layer at high coverages was very close to that of the bulk, and not 10% higher than the bulk, as observed here. Additionally, the butane system is reported to form a crystalline bilayer¹¹ unlike the octane–nonane system where the IQNS data only indicate solid monolayers.

The neutron diffraction measurements also provide an independent estimate of the monolayer compositions, which are in good agreement with IQNS results. The diffraction is also consistent with the hypothesis that no mixed crystal is formed rather patches of pure octane and pure nonane coexist on the surface side-by-side.

Bulk nonane is known to form a rotator phase in the bulk at temperatures very close to the bulk melting point.¹⁵ This is reflected in the transition just below the bulk melting point in Figs. 1 and 2. Rotator phases are reported to be stabilised in mixtures of alkanes and we explain the widening region below the bulk melting point of Fig. 2 in this manner. Pure octane does not show a rotator phase so this feature must disappear before pure octane is reached, and it does.

The rotator phases of bulk alkanes usually occur as the crystal structure tends to a more symmetric hexagonal arrangement of molecules. Evidence for a similar change in symmetry indicating such a transformation was reported here.

The heat capacity peak from the rotator phase is somewhat lower in temperature than for nonane in the absence of graphite. We attribute this displacement to some structural perturbation of the bulk nonane in the pores of the graphite, such that the transition to the rotator phase is shifted to lower temperatures. Depression of bulk melting points in the pores of graphite has been reported elsewhere.^{21,22}

The highest temperature transition of Fig. 5(a) we attribute to melting of the solid monolayer of nonane because this coincides with the loss of translational motion observed in the IQNS data.

We are currently unable to unambiguously identify the lower temperature transitions of the monolayer. There are several possibilities, particularly the formation of monolayer

rotator or hexatic phases. The current diffraction data did not show any clear evidence for such transitions. However, recent diffraction data from dodecane adsorbed onto graphite from its liquid indicate that a solid monolayer with low symmetry is replaced by one with higher symmetry before the monolayer melts.²³

Acknowledgements

The authors thank the instrument scientists and staff at ILL, Grenoble, France. We also thank the UK EPSRC, the Spanish DGICYT, the British Council and the Grant-in-aid for Scientific Research from Monbusho (AI) for financial support. Contribution No. 6 from the Research Centre for Molecular Thermodynamics.

References

- 1 G. H. Findenegg, *J. Chem. Soc., Faraday Trans. 1*, 1972, **168**, 1799.
- 2 G. H. Findenegg, *J. Chem. Soc., Faraday Trans.*, 1973, **169**, 1969.
- 3 H. Kern and G. H. Findenegg, *J. Colloid Interface Sci.*, 1980, **75**, 346.
- 4 A. J. Groszek, *Proc. R. Soc. London, Ser. A*, 1970, **314**, 473.
- 5 G. Fragneto, R. K. Thomas, A. R. Rennie and J. Penfold, *Langmuir*, 1996, **12**, 6036.
- 6 J. P. Rabe and S. Buchholz, *Science*, 1991, **253**, 424.
- 7 M. A. Castro, S. M. Clarke, A. Inaba and R. K. Thomas, *J. Phys. Chem. B*, 1997, **101**, 8878.
- 8 M. A. Castro, S. M. Clarke, A. Inaba, C. C. Dong and R. K. Thomas, *J. Phys. Chem. B*, 1998, **102**, 777.
- 9 M. A. Castro, S. M. Clarke, A. Inaba and R. K. Thomas, *Physica B*, 1998, **241–243**, 1086.
- 10 M. A. Castro, S. M. Clarke, A. Inaba, T. Arnold and R. K. Thomas, *J. Phys. Chem. B*, 1998, **102**, 10528.
- 11 K. W. Herwig, J. C. Newton and H. Taub, *Phys. Rev. B*, 1994, **50**, 15287.
- 12 J. Krim, J. Suzanne, H. Shechter, R. Wang and H. Taub, *Surf. Sci.* 1985, **162**, 446.
- 13 F. Y. Hansen and H. Taub, *Phys. Rev. Lett.*, 1992, **69**, 652.
- 14 S. M. Clarke, A. Inaba, T. Arnold and R. K. Thomas, *J. Therm. Anal. Calorim.*, 1999, **57**, in press.
- 15 K. N. Marsh, *Thermodynamic Properties of Organic Compounds and their Mixtures*, Springer-Verlag, Berlin, 1995.
- 16 E. B. Sirota, H. E. King, H. H. Shao and D. M. Singer, *J. Phys. Chem.*, 1995, **99**, 798.
- 17 P. Espeau, Y. Hagety, M. A. Cuevas-Diarte and H. A. J. Oonk, *Proceedings of the XXI J.E.E.P. Rouen*, 1995.
- 18 A. Wurfinger and G. M. Schneider, *Ber. Bunsen-Ges. Phys. Chem.*, 1973, **77**, 121.
- 19 J. K. Kjems, L. Passell, H. Taub, J. G. Dash and A. D. Novaco, *Phys. Rev. B*, 1976, **13**, 1446.
- 20 B. E. Warren, *Phys. Rev.*, 1941, **59**, 693.
- 21 P. Epseau and J. White, *J. Chem. Soc., Faraday Trans.*, 1997, **93**, 3197.
- 22 P. Epseau, P. A. Reynolds, T. Dowling, D. Cookson and J. White, *J. Chem. Soc., Faraday Trans.*, 1997, **93**, 3201.
- 23 S. M. Clarke, M. A. Castro, A. Inaba, T. Arnold and R. K. Thomas, 1999, unpublished work.
- 24 A. I. Kitaigorodskii, *Mixed Crystals*, ed. M. Cardona, P. Fulde and H.-J. Queisser, Springer-Verlag, Berlin, 1984.

Paper 9/06184C